Journal of Applied Polymer Science

Evaluation of Wool Nanoparticles Incorporation in Chitosan/Gelatin Composite Films

Niloofar Eslahi,[1] Fatemeh Dadashian,[1,2] Nahid Hemmati Nejad,[1] Mohammad Rabiee[3]

[1]Department of Textile Engineering, Amirkabir University of Technology, Tehran, Iran

[2]Center of Excellence on Functional Fibrous Structures and Environmental Enhancement, Amirkabir University of Technology, Tehran, Iran

[3]Department of Biomedical Engineering, Amirkabir University of Technology, Tehran, Iran

Correspondence to: F. Dadashian (E-mail: dadashia@aut.ac.ir)

ABSTRACT: The aim of this work was to develop chitosan/gelatin composite films embedded with various amounts of wool nanoparticles, which were produced by an environmental friendly process. Films loaded with wool nanoparticles were subjected to physiochemical, biological, and mechanical characterization. The obtained results showed that incorporation of wool nanoparticles into chitosan/gelatin composite led to a reduction in swelling, moisture content and dissolution degree of the films. *In vitro* degradation test revealed that the nanoparticles-embedded composites had a lower degradation rate than that of chitosan/gelatin composite. Besides, composite films containing wool nanoparticles showed an improvement in the stability in phosphate buffered saline. On the other hand, tensile strength and elongation at break decreased upon loading the films with wool nanoparticles. The biocompatibility of the produced composites was also confirmed by MTT test. © 2013 Wiley Periodicals, Inc. J. Appl. Polym. Sci. **2014**, *131*, 40294.

KEYWORDS: biopolymers and renewable polymers; properties and characterization; biomaterials; biodegradable; biocompatibility

Received 14 August 2013; accepted 12 December 2013

DOI: 10.1002/app.40294

INTRODUCTION

The new requirements for reducing petroleum-based plastic materials have promoted the use of environmental friendly and biodegradable polymers from renewable resources, as a consequence of the environmental and ecological problems associated with the disposal of these synthetic polymers.[1] Biodegradable films, which have attracted much attention in recent years, are generally made from biopolymers such as proteins, polysaccharides, lipids, or their blends.[2] On the other hand, protein wastes such as by-products from agricultural sources, wool textile industry, poor quality raw wool not fit for spinning, and hair and feathers from butchery constitute an important renewable source of biopolymers.[3] With increasing demand for sustainable materials, these protein by-products also started to be regarded as renewable resources worthy of a better exploitation.[4]

Chitosan is a partially deacetylated derivative of chitin, a natural abundant substance found in the exoskeletons of insects, shells of crustaceans, and fungal cell walls.[5] Chitosan is a copolymer composed of D-glucosamine and *N*-acetyl-D-glucosamine linked through β-(1-4) glycosidic linkages, forming a long linear polymer chain. This polycationic polysaccharide has one amino group and two hydroxyl groups in the repeating glucosidic residue.[6] The molecular weight and the ratio of glucosamine to *N*-acetyl glucosamine, i.e., degree of *N*-deacetylation (DD), are thought to be the two most important determinants of chitosan characteristics.[7] Chemical and biochemical reactivity of chitosan is strongly related to the free primary amine groups distributed regularly through its molecular chain. This promising biopolymer has been extensively used over a wide range of applications due to its high biocompatibility, biodegradability, antimicrobial activity, adsorption, film-forming properties, and low antigenicity.[8,9]

Gelatin is a soluble protein, which can be obtained by hydrolysis of the fibrous insoluble collagen present in the bones and skin generated as waste during animal slaughtering and processing.[10] The characteristic triple-helical structure of collagen is lost during gelatin extraction, but can be recovered below the helix–coil transition temperature.[11] Gelatin can be visualized as a copolymer build-up from triads of α-amino acids with glycine at every third position (soft blocks) and triads of hydroxyproline, proline, and glycine (rigid blocks), with a narrow molar mass distribution.[12] The three-dimensional gel network of gelatin is composed of micro-crystallites interconnected with amorphous regions of randomly coiled segments. This protein is unique among hydrocolloids in forming thermo-reversible with a melting point close to the body temperature, which is particularly significant in edible and pharmaceutical applications.[13] Attractive properties of

© 2013 Wiley Periodicals, Inc.

gelatin such as low cost, good biocompatibility, biodegradability, low immunogenicity, adhesiveness, and bio-absorptivity make it suitable for biomedical development.[7,14]

Although chitosan and gelatin have recognized properties to be applied in different fields, they have also some drawbacks that restrict their end use due to their inherent hydrophilic character. A promising strategy to overcome such limitations is through blending.[12,15] The backbone of gelatin contains free negatively charged carboxyl groups, enabling it to blend with the cationic ammonium groups of chitosan to form a network.[16] Composite films of chitosan and gelatin have been reported to have improved mechanical, transport, physical, and biological properties as compared with those of single components.[17–20] This was attributed to the formation of polyelectrolyte complexes (PECs) through electrostatic interactions between them at suitable pH.[18,21] Besides, the presence of arginine-glycine-aspartic acid (RGD) sequence in gelatin promotes cell adhesion, migration, differentiation, and proliferation.[22]

Wool, a biopolymer obtained from the fleece of sheep, is basically composed of the fibrous protein, keratin, which is regarded as three-dimensional polymer interlinked by intermolecular bonding of disulfide cystine amino acid and inter- and intramolecular bonding of polar and nonpolar amino acids leading to its high stability and distinctive physical characteristics.[3,4,23] Like many naturally-derived biomolecules, keratin has intrinsic biological activity and biocompatibility. Even though keratins have high potential for a number of applications, their usage is rather limited because of their poor mechanical properties. An alternative solution is blending with other natural biopolymers to improve their properties.[24–26] However, in most of these studies, keratin was extracted chemically, and the obtained keratin solution was then used for film/scaffold fabrication. Solution routes have inherent bottlenecks in the preparation process, such as long time of dialysis, high production costs, safety, and environmental constraints.[27] Since, the protein powder could keep the original properties of the material without destroying the microstructure, it has been widely applied in modern industries. However, production of particles from protein fibers was mostly performed by harsh chemical or mechanical processes.[28]

As a consequence, in this study, to integrate the advantages of chitosan, gelatine, and wool nanoparticles, preparation of composite films was investigated. In other words, chitosan/gelatin composite films were embedded with wool nanoparticles, which were produced by enzymatic hydrolysis, an environmental friendly technique, followed by ultrasonic treatment, and their physiochemical and mechanical properties, stability, biodegradability, and biocompatibility were evaluated.

EXPERIMENTAL

Materials

Gelatin (for microbiology) and glycerol (98% reagent grade) were supplied by Merck Co. (Germany). Chitosan (medium molecular weight) and hen egg white lysozyme (50,000 U/mg) were provided by Sigma-Aldrich (USA). All other chemicals used such as acetic acid, tris base, sodium acetate, and sodium hydroxide were of analytical grade. Waste wool fibers, collected from spinning process, was originated from New Zealand Merino wool with a mean diameter of 21 μm. Wool nanoparticles were produced from these fibers by enzymatic hydrolysis followed by ultrasonic treatment, as it was reported previously.[29] The number-based particle size distribution gave an average particle size of 137 nm with 90% of the particles being less than 150 nm in size.

Films Preparation

All films were obtained by casting from their film forming solutions. Two percent (w/v) of chitosan and gelatin solution was prepared separately by dissolving in 1% acetic acid aqueous solvent and deionized water, respectively, at 50°C until homogenization. Glycerol was added to each solution as a hydrophilic plasticizer at a concentration of 25 wt % (based on polymers dry weight). Incorporation of glycerol into natural polymer films eliminates their fragility and improves their flexibility. Plasticizers by reducing the intermolecular forces soften the rigidity of the film structure and increase the mobility of the biopolymer chains, thus improving the mechanical properties.[2,12,30,31] The prepared solutions were filtered and 25 mL of each solutions were poured separately into polystyrene Petri dish, allowed to dry at room temperature, peeled off from the plates, washed with 80% ethanol until the films were neutral and finally dried in a vacuum oven for 20 min.

For composite films, gelatin solution with or without wool nanoparticles (0.1, 0.3, and 0.5% w/v) was added drop-wise to the chitosan solution at 1 : 1 ratio (w/w), the acidity of the resulting mixture was adjusted to pH = 5.5 with 1*M* NaOH, then stirred for 2 h at 50°C, followed by casting and evaporation as described above. According to the literature, it was shown that the polyelectrolyte complex between chitosan and gelatin can only occur at the pH above the isoelectric point of gelatin ($pH_{iso} = 4.7$), where gelatin chains are negatively charged, and below pH 6.2, to prevent chitosan precipitation out of solution.[18] The resulting composite films were labeled CHG, CHGNW0.1, CHGNW0.3, and CHGNW0.5 as chitosan/gelatin composite films without and with wool nanoparticles; the numbers after CHGNW designating the percentage of the nanoparticles in the chitosan/gelatin composites.

FILM CHARACTERIZATION

Analyses

Microstructure was examined by SEM on Philips (XL30) with an operating voltage of 20 kV after gold coating. The surface and cross section (cryofractured in liquid nitrogen) of the films were observed under the microscope. FTIR spectra of the films were carried out on a Nicolet Nexus 670 using KBr pellets. The characteristic spectra were scanned in the wave number range of 4000 to 400 cm^{-1} at a resolution of 4 cm^{-1}. The crystalline behavior of the membranes was also investigated using XRD Equinox 3000 (INEL, France) equipped with Cu-Ka radiation source ($\lambda = 0.154$ nm). The samples were scanned from $2\theta = 5°$ to 40°. Moreover, DSC analysis was performed with DSC 2010 (TA Instruments, USA) at a heating rate of 10°C/min within the range of 0 to 300°C in flowing nitrogen atmosphere.

Mechanical Test

To evaluate the mechanical properties of the films, experiments were carried out on an Instron 5566 at a crosshead speed of 25

mm/min according to ASTM D882-02. Film probes of 10 cm length and 2.5 cm width were used. Before analysis, the films were stored at 23 ± 2°C and 60 ± 5% relative humidity (RH) for at least 48 h. The thickness of the membrane was measured using a manual micrometer with an accuracy of 0.01 mm and cross-sectional area was calculated. Tensile strength (TS) was determined by dividing the required force for film rupture by the area of the transverse section, elongation at break was also calculated from the ratio of increase in length to original length, expressed in percentage and the results were given as the arithmetic means of three different samples.[15]

Swelling

The swelling characteristics of the films were determined by swelling films with known weights in acetate buffer (pH = 4), PBS (pH = 7), and Tris-HCl (pH = 9) for 24 h to achieve complete saturation. The films were then withdrawn and their wet weights were determined after removing surface water by blotting with a filter paper. The swelling ratio of the films was calculated by the following equation:

$$\mathrm{SW} = \frac{w_s - w_d}{w_d} \times 100 \quad (1)$$

where W_d and W_s are, respectively, the weights of the films in the dry and swollen states.

Moisture Content and Total Soluble Matter

The specimens of each film were weighed (m_0) and subsequently dried in an oven at 100°C for 24 h. Films were then reweighed (m_d), to determine their moisture content (MC):

$$\mathrm{MC}\,(\%) = \frac{m_o - m_d}{m_o} \times 100 \quad (2)$$

Total soluble matter (TSM) was measured by immersing the dried samples in 10 mL of distilled water at room temperature for 24 h. After this time, specimens were dried again at 100–105°C for 24 h to determine the weight of dry matter not dissolved in water. TSM was determined as the weight difference between the initial dry matter (W_1) and the undissolved dry matter after immersion (W_2), and expressed as a percentage of the initial dry matter.[2]

$$\%\mathrm{TSM} = \frac{w_1 - w_2}{w_1} \times 100 \quad (3)$$

Stability

Air-dried films were first weighed accurately and then immersed in PBS (pH = 7) at 37°C for intervals from 1 day up to 10 days. Films were then removed and a second weighing was conducted to determine the stabilities of the films by determining their weight loss after blotting them with a filter paper to remove the adsorbed water. Stability of the films in the aqueous solution is expressed by the following equation:

$$\mathrm{ST} = \frac{w_2}{w_1} \times 100 \quad (4)$$

where W_1 and W_2 are the weights of films before and after the test, respectively.[14]

In Vitro Biodegradation

The biodegradation study was carried out *in vitro* by incubating films in PBS (pH = 7) containing 10^4 U/mL lysozyme at 37°C. Films were removed from the medium at regular intervals from 1 day up to 10 days and dried. The degree of degradation is expressed as percentage of weight loss (D) as follows:

$$\mathrm{D} = \frac{w_o - w_t}{w_o} \times 100 \quad (5)$$

where W_0 denotes the original weight and W_t is the weight at time t.[22] All above experiments were repeated three times and the average values were reported.

Cell Proliferation

Cytotoxicity testing of the films was evaluated according to ISO 10993-5 using dimethylthiazol diphenyl tetrazolium bromide (MTT) assay. This test is based on the fact that active cells convert the yellowish MTT to an insoluble purple formazan crystal. The formazan crystals formed are solubilized and the resulting colored solution is quantified using a spectrophotometer.[32] Films were firstly sterilized by immersing in excess 70% ethanol solution for 30 min and kept under UV for 1 h. The samples then dried in vacuum oven and washed with sterile PBS at least five times prior to use. To prepare the extracts for each film, the samples were incubated in 1 mL of RPMI 1640 culture medium (Sigma) supplemented with 10% (w/w) fetal bovine serum (FBS, GIBCO, Scotland) under shaking conditions for 5 and 10 days. Pure culture medium (RPMI and FBS) kept under similar conditions was used as a control sample.

Following extraction, L929 fibroblast cells were harvested into 96-well tissue culture plates at density of 1×10^4 cells/well and incubated at 37°C for 24 h. In the next step, the culture medium in each well was replaced with 90 μL of extraction media together with 10 μL FBS and was incubated for another 24 h. Then, the extraction fluids were changed with MTT (Sigma) solution (0.5 mg/mL) and the plates were incubated for 4 h at 37°C. The purple formazan crystals were detected and were dissolved by the addition of 100 μL of isopropanol (Sigma, USA) per well. After 15 min slow shaking, the optical density was measured at the wavelength of 545 nm by using a multiwell microplate ELISA reader (ICN, Switzerland). The results were normalized with respect to the control sample.

Statistical Analysis

Data values obtained in the experiments were statistically analyzed by one-way analysis of variance (ANOVA) employing SPSS 15 software. Differences in the properties of the films were determined by Fisher's least significant difference (LSD) mean discrimination test, using $P < 0.05$ as level of significance.

RESULTS AND DISCUSSION

SEM

The surface micrographs of chitosan, gelatin, and composite films in Figure 1 reveal clean and smooth matrix without any pores. The cross-sections also show homogeneous surfaces with excellent structural integrity. Composite film of gelatin and chitosan is also characterized by a compact, uniform, dense, and homogenous appearance. It is worth noting that no interfaces are observed in the blend indicating a high compatibility between components due to associative interactions to form polyelectrolyte complex (PEC).[33]

SEM images of wool nanoparticles-embedded chitosan/gelatin composite in Figure 2 depict that wool nanoparticles are rather

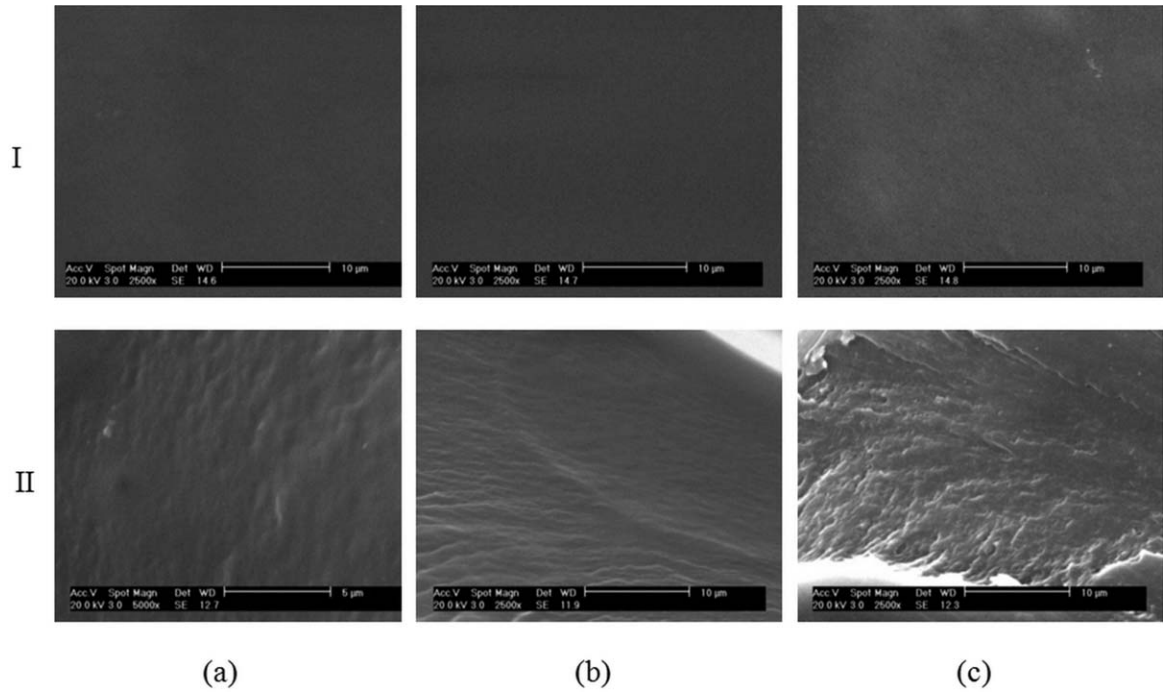

Figure 1. (I) Surface morphology and (II) cross-sections of (a) chitosan, (b) gelatin, and (c) chitosan/gelatin composite films.

uniformly distributed in the composite. However, some aggregates of the nanoparticles are observed as the amount of particles increase. In addition, incorporation of wool nanoparticles leads to a more compact, aggregated and irregular structure than the composite film in Figure 1(c).

FTIR

The FTIR spectra of the films are shown in Figure 3. The spectrum of pure chitosan exhibits a broad absorption band in the 3500–3400 cm^{-1} with a maximum at 3410 cm^{-1} results from overlapping of the O—H and N—H stretching vibrations of

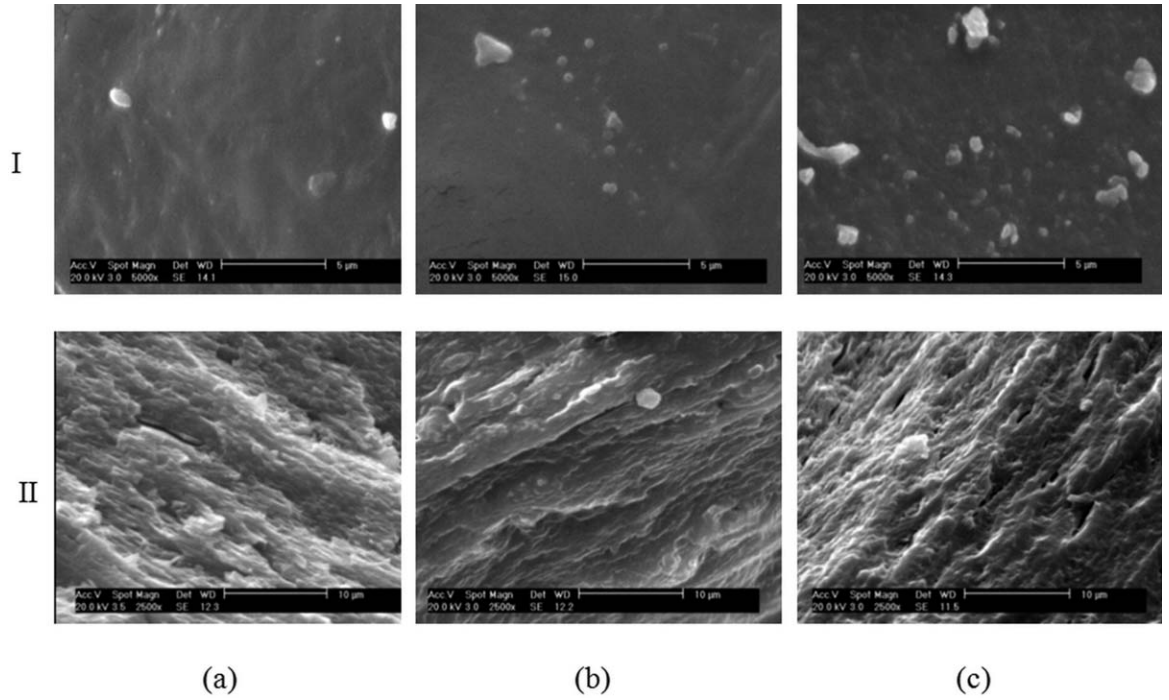

Figure 2. SEM images of chitosan/gelatin composite films containing (a) 0.1%, (b) 0.3%, and (c) 0.5% wool nanoparticles. Top images (I) show surface morphology and the bottom ones (II) show the cross-sections.

functional groups engaged in hydrogen bonds. The peaks around 2925 and 2860 cm^{-1} are assigned to —CH_2 and —CH_3 groups (aliphatic group) of carbohydrate ring. The sharp peak at 1410 cm^{-1} is assigned to the CH_3 symmetrical deformation mode and OH vibration, 1154, 1087, and 1029 cm^{-1} correspond to the bridge oxygen (C—O—C) stretching bands, characteristics of chitosan saccharide structure.[34,35] The spectrum also exhibits the distinctive absorption bands at 1637 and 1564 cm^{-1}, which are the characteristic peaks of the amide I and amide II (—CH_3—C═O group, denoting the presence of the acetyl group), respectively. The shoulder at 1637 cm^{-1} suggests that chitosan comes from a high deacetylation process. Residues of chitin, attributed to N—H bond of N-acetyl group (amide II) were evidenced by the peak at 1564 cm^{-1}.[12,36]

The spectra of gelatin film display relevant peaks arisen from C═O stretching at 1647 cm^{-1} (amide I), N—H bending at 1541 cm^{-1} (amide II) and C—N stretching and N—H in plane bending at 1240 cm^{-1} (amide III).[18,33] The peak situated around 1082 cm^{-1} might be related to the interactions arising between plasticizer (OH group of glycerol) and gelatin by hydrogen bonding.[37] Besides, the broad absorption band in the region of 3500–3200 cm^{-1} is attributed to the N—H stretching of the amino groups (amide A), which must be masked by the absorption peak due to O—H groups.[12]

The spectrum of the composite exhibits the characteristic peaks of both chitosan and gelatin with slight differences in some regions. Incorporation of gelatin into chitosan shifts the carbonyl and amino bands of chitosan, i.e., from 1637 to 1652 cm^{-1} and from 1564 to 1553 cm^{-1}, respectively, which implies hydrogen bonding networks between polymer molecules in the polyelectrolyte complex formation.[19] The spectrum of chitosan/gelatin film shows that C═O groups of the gelatin interacted

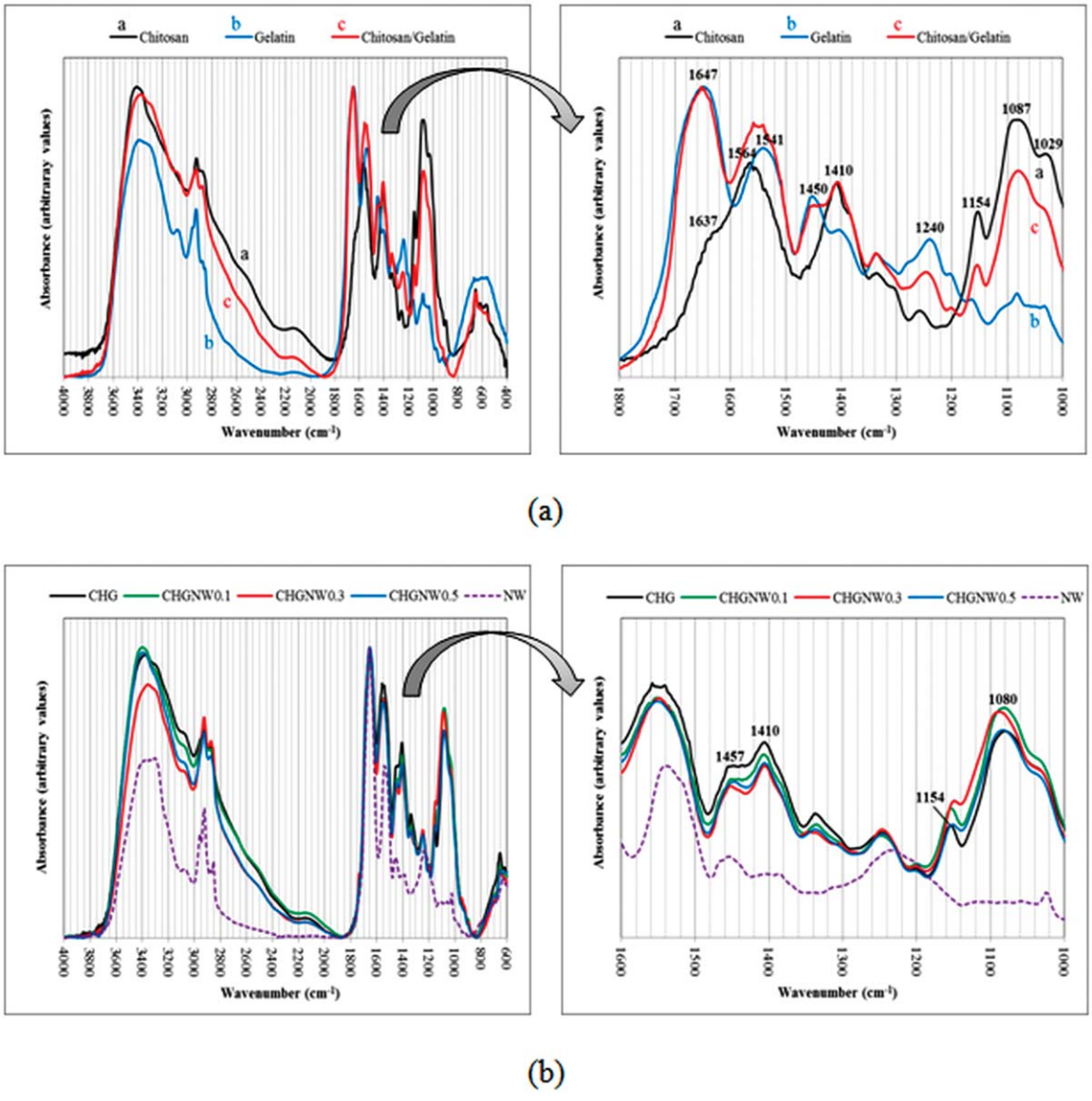

Figure 3. FTIR spectra of (a) chitosan, gelatin, and chitosan/gelatin films, and (b) composite films with or without wool nanoparticles. [Color figure can be viewed in the online issue, which is available at wileyonlinelibrary.com.]

with N—H groups of chitosan, results in the increased carbonyl stretching at 1650 cm^{-1} and the decreased C—O—C bridge stretching vibration of chitosan at 1080 and 1154 cm^{-1}. In fact, O—H groups of chitosan interacted with COOH groups of gelatin, reducing C—O stretching bands of chitosan saccharine structure.[14] Besides, the composite film has a slight shift to the lower wavenumber of amide A (from 3389 cm^{-1} in gelatin and 3410 cm^{-1} in chitosan to 3376 cm^{-1} in composite), possibly due to some alterations in hydrogen bonding.[33] These small modifications suggest specific chemical interactions between chitosan and gelatin molecular chains and may be related to the formation of an interpenetrating polymeric network without any significant changes in their chemical properties.

Composite films containing wool nanoparticles (CHGNW) depict nearly similar characteristic peaks to chitosan/gelatin composite. However, there are some slight changes in the intensity of amides and saccharine regions because of the presence of the nanoparticles in the blends. Addition of nanoparticles to PEC composite leads to an increase in C—O stretching vibration at 1080 and 1154 cm^{-1}. Besides, the C—N stretching vibration at 1457 cm^{-1} arising from interactions of chitosan with gelatin is reduced indicating that the functional groups of chitosan in the nanoparticles-embedded composite interacted with carboxyl groups of gelatin less than those of chitosan in the chitosan/gelatin composite film. However, the existence of wool nanoparticles in the composite does not prevent the interactions between chitosan and gelatin to form PEC. The obtained results indicate that no chemical reaction has occurred between wool nanoparticles and chitosan/gelatin complex; only physical mixture of the constituents happened.

XRD

Chitosan film is characterized by crystalline peaks at $2\theta = 18.9°$, 16.6°, 12.0°, and 8.9° in Figure 4, while the broad peak centered at $2\theta = 23°$ indicates the existence of an amorphous structure.[12,38] Peaks at 12° and 23° are the typical fingerprints for chitosan and are attributed to the 020 diffraction plane of anhydrous chitosan crystal and to the 110 diffraction plane, respectively.[39,40] The new peaks in plasticized-chitosan are assigned to the 020 diffraction plane of hydrated chitosan crystals and related to the films preparation procedure, i.e., dissolution of chitosan in an acetic acid solution.[41,42]

The diffractogram of gelatin film shows two diffraction peaks at ~8.5° and 20.4°. According to Bigi et al., the peak at 2θ around 8.5° is related to the diameter of the triple helix, and its intensity is associated with the triple-helix content of the gelatin films.[43] Besides, the large broad band centered at about 20° corresponds to the amorphous phase.[7,12] Bergo et al. suggested that the amorphous character of the gelatin films containing glycerol was due to the lack of recrystallization and semicrystalline regions during film production.[37]

If chitosan and gelatin have low compatibility, each polymer would have its own crystal region in the blend. However, in XRD pattern of the composite film, the diffraction peaks of chitosan almost disappear and the intensity of the diffraction peaks at about 9° as well as 19° decreases greatly and becomes broad, illustrating that the presence of gelatin reduces the crystallinity of

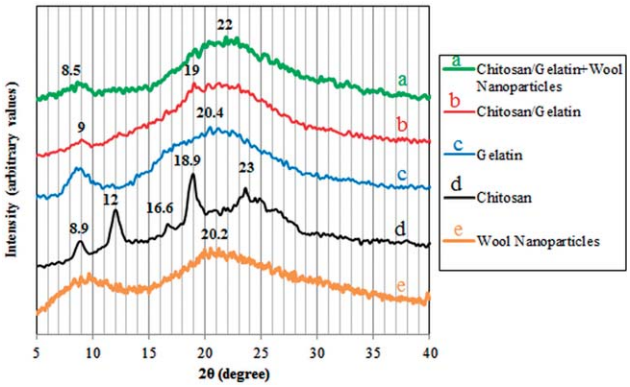

Figure 4. X-ray diffraction curves of different films as well as wool nanoparticles. [Color figure can be viewed in the online issue, which is available at wileyonlinelibrary.com.]

chitosan and therefore the composite tend to become amorphous. This phenomenon is due to the strong interaction between chitosan and gelatin, in line with FTIR results.[21,44,45] The decreased crystallinity of the composite film is mainly attributed to the broken hydrogen bonding in the chitosan molecules, which destroys its intrinsic crystalline structure. When a polyelectrolyte complex forms, amino groups in chitosan form hydrogen bonding with carboxyl groups in gelatin, which results in an amorphous structure of the composite implying their good compatibility.[19,20]

Wool nanoparticles show the typical diffraction pattern of α-keratins with a prominent 2θ peak at 20.2° and a minor peak at about 10°.[46] The XRD pattern of the composite film with 0.3% wool nanoparticles shows almost similar pattern to composite film indicating almost no significant changes in the crystalline structure of the chitosan/gelatin film.

DSC

DSC plots of different films are presented in Figure 5. The first transition for chitosan film started at 63.3°C with a peak at 90.8°C, associated with dehydration of water molecules, followed by the crystalline melting endothermic peak around 170°C, and the exothermic peak at 279.4°C, ascribed to the polymer decomposition including dehydration of the saccharide rings, depolymerization, and decomposition of the acetylated and deacetylated units of chitosan.[35,47] In gelatin film, water evaporation and helix–coil transition (T_m) are observed as endothermic peaks around 90.1 and 204.3°C, respectively.[43,48] The enthalpy for the first endothermic peak represents the energy required to vaporize the water present in the films. The higher evaporation enthalpy (357.1 J/g) in gelatin indicates that water molecules are strongly bound as compared with chitosan (304.6 J/g). Several authors attribute this endothermic peak to the overlapping of different process such as water evaporation, melting, and recrystallization of small and/or imperfect gelatin crystallites, and association of the glass transition of α-amino acid blocks in the polypeptide chain, which are strongly related to film drying conditions.[49–52]

The PEC film prepared in the present study exhibits two endothermic peaks and an exothermic one as well. The first transition in composite film, related to the volatilization of absorbed water,

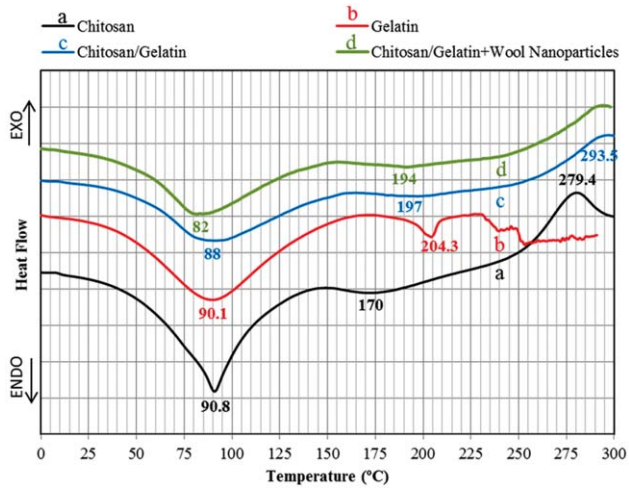

Figure 5. DSC curves of chitosan, gelatin, and chitosan/gelatin composite films with and without wool nanoparticles. [Color figure can be viewed in the online issue, which is available at wileyonlinelibrary.com.]

shifts towards lower temperature with respect to those of each individual components, which is an evidence of intermolecular hydrogen bonding in the polyelectrolyte complex formation. The second endothermic peak is probably associated with the cleavage of the electrostatic interactions between the oppositely charged polymers[53] and the onset temperature is situated about 175°C with a weak peak at 197°C. It is worth noting that the temperature of the second endothermic peak (thermal denaturation of triple-helix) in gelatin almost disappeared upon blending with chitosan, which suggests that the presence of chitosan alters the formation of the characteristic helical structure of gelatin probably by disrupting the hydrogen bonds between gelatin chains.[54] Furthermore, chitosan/gelatin membrane has higher thermal stability than chitosan film. The composite shows thermal degradation at 293.5°C, while the chitosan membrane shows at 279.4°C. It is due to the formation of strong interactions between gelatin and chitosan leading to their good miscibility.[5] In contrast, the gelatin film is thermally less stable than the composite. The amorphous gelatin degrades faster (230°C) than the chitosan/gelatin membrane.

The endothermic peaks in chitosan/gelatin film shift slightly towards lower temperature upon blending with 0.3% wool nanoparticles, which might be due to the reduction in the interactions between chitosan and gelatin with addition of nanoparticles.

Tensile Properties

Mechanical properties of films are largely associated with distribution and density of inter- and intramolecular interactions in the composite network. Table I summarizes the mechanical parameters obtained from stress–strain curves. Gelatin film exhibits an average TS of 16.55 MPa, which increases significantly ($P < 0.05$) upon blending with chitosan up to 26.67 MPa. The obtained results suggest interactions between gelatin and chitosan via hydrogen bonds and the formation of complex with oppositely charged ionic polymers, giving rise to film strengthening.[33,41]

In the composite film, the statistically significant reduction in TS and increase in strain of chitosan might be attributed to the presence of gelatin that reduces the crystallization capacity of chitosan in the film, as confirmed by XRD patterns. These results show that mechanical properties of chitosan can be improved by blending with gelatin. In fact, a soft and elastic complex can be formed, which would be suitable for various applications.

Table I. Mechanical Properties of Different Films

Sample	Tensile Strength (MPa)	Elongation at Break (%)
Gelatin	16.55 ± 1.06^{a}	26.04 ± 1.84^{a}
Chitosan	32.58 ± 3.32^{b}	11.25 ± 2.83^{b}
CHG	26.67 ± 0.90^{c}	42.71 ± 1.11^{c}
CHGNW0.1	24.91 ± 0.51^{d}	38.54 ± 2.06^{d}
CHGNW0.3	23.37 ± 0.23^{e}	31.04 ± 0.45^{e}
CHGNW0.5	19.92 ± 0.30^{f}	31.25 ± 0.67^{e}

Any two means in the same column followed by the same superscript letter are not significantly ($P > 0.05$) different.

It is also observed that with the addition of nanoparticles, tensile strength, and elongation of the blended films decrease, particularly at high nanoparticle content (0.5%), which is probably due to the irregular microstructure of the embedded composites and the aggregation of the nanoparticles. However, elongation values of composite films containing 0.3% and 0.5% wool nanoparticles did not differ significantly ($P > 0.05$).

Swelling

The swelling ratios of the membranes in acetate buffer (pH = 4), PBS (pH = 7), and Tris-HCl (pH = 9) after 24 h immersion are shown in Figure 6. It should be mentioned that chitosan films almost dissolve at pH = 4. In addition, gelatin is soluble in aqueous solution and a few hours of storage in buffer solutions induce noticeable swelling, which makes it too weak to take out from the swelling buffer to measure its weight. The chitosan/gelatin composite film shows significantly ($P < 0.05$) lower swelling percentage than the individual films, which might be due to the strong hydrogen bonds between gelatin and chitosan in the polyelectrolyte complex. Thus, this composite

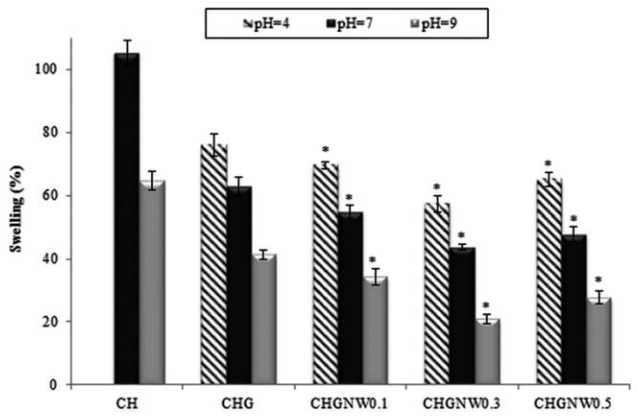

Figure 6. Swelling ratio of different films in different pH solutions after 24 h at room temperature. Error bars correspond to standard deviation. $^{*}P < 0.05$ relative to chitosan/gelatin composite film.

Table II. Moisture Content and Total Soluble Matter of Different Films

Sample	Moisture Content (%)	Total Soluble Matter (%)
Gelatin	12.67 ± 0.8^a	100 ± 0.0^a
Chitosan	10.17 ± 0.5^b	8.36 ± 2.3^b
CHG	11.13 ± 0.6^c	17.32 ± 0.4^c
CHGNW0.1	9.38 ± 0.4^b	16.02 ± 0.6^d
CHGNW0.3	8.36 ± 0.6^d	13.59 ± 0.5^e
CHGNW0.5	8.74 ± 0.5^d	14.81 ± 0.7^f

Any two means in the same column followed by the same superscript letter are not significantly ($P > 0.05$) different.

film possesses improved waterproof characteristics as compared to the original gelatin and chitosan film.

It is worth noting that almost all films swell more at lower pH because of chitosan high swelling. In fact, the degree of swelling is dependent on pH values in the aqueous solution. This pH-dependent characteristic is promising for biomedical applications such as controlled drug delivery, skin substitute, and biomedical separation systems.[14,22] Chitosan is a basic carbohydrate carrying amino groups whose pK_a is 6.5–7.[55] Therefore, chitosan is positively charged at pH = 4, leading to the extensive swelling because of the repulsion between carbohydrate chains. On the contrary, at pH = 9, uncharged chitosan results in suppression of swelling.[25]

The incorporation of wool nanoparticles in the chitosan/gelatin composite film leads to a significant decrease ($P < 0.05$) in swelling. It is hypothesized that hydrogen interactions between the components reduce water uptake, since polar-side-chain groups become less exposed to bind water. It can be also envisaged that minimum swelling ratio has occurred in composite film containing 0.3% wool nanoparticles among the produced films. The compact structure of this nanoparticles-embedded composite suppresses the water absorption and this is considered advantageous for biomedical applications, since the biomaterials are mostly surrounded by body fluids.

Moisture Content and Solubility

Moisture content is a parameter related to the total void volume occupied by water molecules in the network microstructure of the film, while solubility is related to the hydrophilicity of the material.[12,56] On the basis of the results given in Table II, gelatin film exhibits the highest moisture content, while the lowest value is observed for composite film containing 0.3% wool nanoparticles. TSM value is a measure of the resistance of films against water.[57] Gelatin films are completely soluble in water in accordance with the data given in Refs. 10 and 58. Composite films are significantly less soluble than gelatin, which could result from interactions such as electrostatic forces between positively charged chitosan and negatively charged gelatin at the operating pH (5.5). It is interesting to note that the films containing wool nanoparticles show significantly ($P < 0.05$) lower solubility comparing to the native membrane. In other words, the hydrophilicity of these films is reduced by addition of the nanoparticles.

Stability and Biodegradation Properties

Figure 7(a) shows the degree of stability obtained from different films in PBS (pH = 7) for a 10-day period. Within a few hours, gelatin film almost dissolves; therefore this film is not tested later on. Maximum reduction in stability is observed in the first 4 days for all films, and then it slows down. Chitosan/gelatin composite is much more stable than gelatin film due to the formation of polyelectrolyte complex, but shows lower stability comparing to chitosan film. The films containing wool nanoparticles show higher stability than the native films and the highest stability is also observed for 0.3% wool nanoparticles-embedded chitosan/gelatin composite.

To evaluate the degradation behavior *in vitro*, films were incubated in PBS containing lysozyme for 10 days. Incubated films show maximum weight reduction after 4 days with less significant changes in later time periods. As shown in Figure 7(b), degradation of chitosan-gelatin complex is greater than that of chitosan membrane probably because of the loss of gelatin in the former. As a hydrophilic polymer, gelatin macromolecular chains hydrolyze quickly with the existence of water.[20]

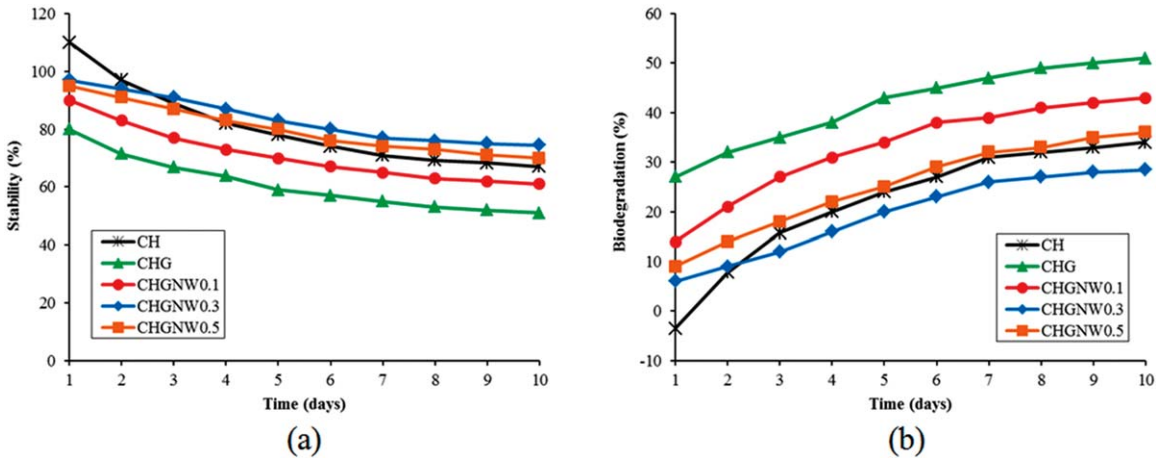

Figure 7. (a) The stabilities of films in PBS and (b) biodegradation of films in the presence of lysozyme for 10 days. [Color figure can be viewed in the online issue, which is available at wileyonlinelibrary.com.]

Degradation of chitosan by lysozyme, which exists in various human body fluids and tissue, involves protonation of amino groups and mechanical relaxation of coiled chitosan chains. The N-acetyl-glucosamine groups of chitosan chains can be hydrolyzed by lysozyme. Owing to the hydrophilic nature of chitosan, the diffusion of water into chitosan matrix is faster than degradation, and the matrix begins to swell prior to degradation.[17,59] As for the films containing wool nanoparticles, lower degradation can be seen comparing to the composite film, particularly for the one with 0.3% wool nanoparticles. In fact, the loaded nanoparticles can play as a hindrance for enzymatic hydrolysis of the film and as a result restrict its biodegradation.

Cell Proliferation Assay

Reduction of MTT reagent is assessed as an assay of mitochondrial redox activity of cultured cells. MTT reagent is a pale yellow substance that is reduced to a dark blue formazan product when incubating with viable cells by mitochondrial succinate dehydrogenase. Therefore, the production of formazan can reflect the level of cell viability on the material.[20] Figure 8 represents the results of the percentage cell viability for different films. As can be seen, the cell viability on gelatin film is similar to the control plate. Gelatin is composed of a series of amino acids, such as arginine, glycin, aspartic acid (RGD sequence), that promotes cell adhesion and migration. A nonspecific cell interaction also exists between chitosan positively charged ammonium sites at physiological pH and negatively charged cell membrane surfaces. As a result, the composite film of chitosan and gelatin seems to be favorable for cell adhesion and the biological activity of chitosan improves upon blending with gelatin.[60]

No statistical difference in cells viability is observed between chitosan/gelatin film and the individual components, but the number of cells reduces significantly ($P < 0.05$) in composite film containing wool nanoparticles in comparison with chitosan/gelatin composite, which might be due to the decrease in the hydrophilicity. However, the slightly higher number of cells on the films surface at the end of the culture period (after 10 days) suggests their good affinity and biocompatibility for cells.

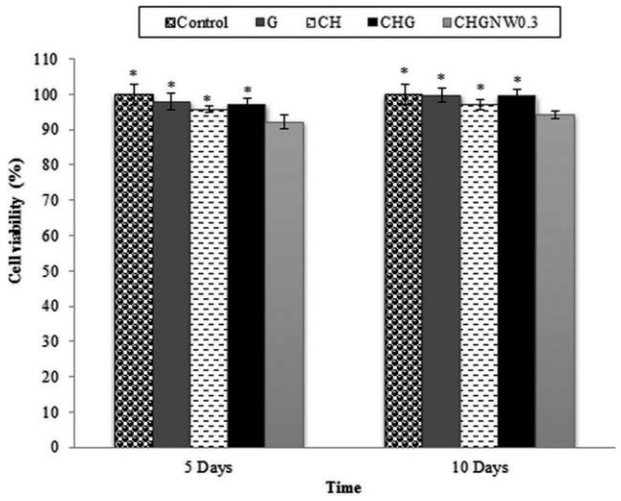

Figure 8. The fibroblast cell viability results for different films. Error bars correspond to standard deviation. $^{*}P < 0.05$ relative to chitosan/gelatin composite film containing 0.3% wool nanoparticles.

CONCLUSIONS

Wool nanoparticles, which were produced by enzymatic hydrolysis followed by ultrasonic treatment, were incorporated in chitosan/gelatin composite to investigate their impact on the properties of the composite films. On the basis of the obtained results of FTIR, XRD, and DSC, the existence of specific interactions between amino groups of chitosan and carboxyl groups of gelatin and as a result formation of a polyelectrolyte complex even in the presence of the wool nanoparticles was confirmed. SEM images showed that the nanoparticles-embedded composites had irregular, rough, and compact microstructure. Tensile strength as well as elongation at break decreased in the composites containing wool nanoparticles due to the destruction of structural regularity and molecular integrity. It was found that this reduction intensified with increasing nanoparticles percentage in the composites. Moreover, the obtained results revealed that minimum swelling, moisture content, solubility, and biodegradation rate occurred in composite with 0.3% wool nanoparticles in comparison with the other ones. Biocompatibility of the composite films in the absence or presence of the nanoparticles was also approved by MTT assay. In conclusion, the wool nanoparticles-embedded chitosan/gelatin composites can be used in a wide range of applications such as food packaging and biomedical industries.

ACKNOWLEDGMENTS

The authors thank the personnel of Cell Bank of Iran Pasteur Institute for their cooperation and useful consultation on biological assay.

REFERENCES

1. Tharanathan, R. N. *Trends Food Sci. Technol.* **2003**, *14*, 71.
2. Leceta, I.; Guerrero, P.; de la Caba, K. *Carbohydr. Polym.* **2013**, *93*, 339.
3. Eslahi, N.; Dadashian, F.; Hemmati Nejad, N. *Prep. Biochem. Biotechnol.* **2013**, *43*, 624.
4. Zoccola, M.; Aluigi, A.; Tonin, C. *J. Mol. Struct.* **2009**, *938*, 35.
5. Nagahama, H.; Maeda, H.; Kashiki, T.; Jayakumar, R.; Furuike, T.; Tamura, H. *Carbohydr. Polym.* **2009**, *76*, 255.
6. Dash, M.; Chiellini, F.; Ottenbrite, R. M.; Chiellini, E. *Prog. Polym. Sci.* **2011**, *36*, 981.
7. Thein-Han, W. W.; Saikhun, J.; Pholpramoo, C.; Misra, R. D. K.; Kitiyanant, Y. *Acta Biomater.* **2009**, *5*, 3453.
8. Ravi Kumar, M. N. V. *React. Funct. Polym.* **2000**, *46*, 1.
9. Pillai, C. K. S.; Paul, W.; Sharma, C. P. *Prog. Polym. Sci.* **2009**, *34*, 641.
10. Gennadios, A. In Protein-Based Films and Coatings; Gennadios, A., Ed.; CRC Press: New Jersey, **2002**; pp 1–41.
11. Yakimets, I.; Wellner, N.; Smith, A. C.; Wilson, R. H.; Farhat, I.; Mitchell, J. *Polymer* **2005**, *46*, 12577.
12. Pereda, M.; Ponce, A. G.; Marcovich, N. E.; Ruseckaite, R. A.; Martucci, J. F. *Food Hydrocolloid.* **2011**, *25*, 1372.
13. Achet, D.; He, X. W. *Polymer* **1995**, *36*, 787.

14. Kim, S.; Nimni, M. E.; Yang, Z.; Han, B. *J. Biomed. Mater. Res. Part B* **2005**, *75B*, 442.
15. Rivero, S.; García, M. A.; Pinotti, A. *J. Food Eng.* **2009**, *90*, 531.
16. Taravel, M. N.; Domard, A. *Biomaterials* **1993**, *14*, 930.
17. Huang, Y.; Onyeri, S.; Siewe, M.; Moshfeghian, A.; Madihally, S. V. *Biomaterials* **2005**, *26*, 7616.
18. Yin, Y.; Li, Z.; Sun, Y.; Yao, K. *J. Mater. Sci.* **2005**, *40*, 4649.
19. Cheng, M.; Deng, J.; Yang, F.; Gong, Y.; Zhao, N.; Zhang, X. *Biomaterials* **2003**, *24*, 2871.
20. Zhuang, H.; Zheng, J.; Gao, H.; Yao, K. *J. Mater. Sci.: Mater. Med.* **2007**, *18*, 951.
21. Yin, Y. J.; Yao, K. D.; Cheng, G. X.; Ma, J. B. *Polym. Int.* **1999**, *48*, 429.
22. Mao, J. S.; Zhao, L. G.; Yin, Y. J.; Yao, K. D. *Biomaterials* **2003**, *24*, 1067.
23. Cardamone, J. M. *J. Mol. Struct.* **2010**, *969*, 97.
24. Balaji, S.; Kumar, R.; Sripriya, R.; Kakkar, P.; Ramesh, D. V.; Reddy, P. N. K.; Sehgal, P. K. *Mater. Sci. Eng. C* **2012**, *32*, 975.
25. Tanabe, T.; Okitsu, N.; Tachibana, A.; Yamauchi, K. *Biomaterials* **2002**, *23*, 817.
26. Thilagar, S.; Jothi, N. A.; Omar, A. R. S.; Kamaruddin, M. Y.; Ganabadi, S. *J. Biomed. Mater. Res. Part B* **2009**, *88B*, 12.
27. Rajkhowa, R.; Zhou, Q.; Tsuzuki, T.; Morton, D. A. V.; Wang, X. *Powder Technol.* **2012**, *224*, 183.
28. Xu, W.; Wang, X.; Li, W.; Peng, X.; Liu, X.; Wang, X. G. *Macromol. Mater. Eng.* **2007**, *292*, 674.
29. Eslahi, N.; Dadashian, F.; Hemmati Nejad, N. *Adv. Powder Technol.* **2013**, *24*, 416.
30. Jongjareonrak, A.; Benjakul, S.; Visessanguan, W.; Tanaka, M. *Eur. Food Res. Technol.* **2006**, *222*, 229.
31. López-Caballero, M. E.; Gómez-Guillén, M. C.; Pérez-Mateos, M.; Montero, P. *Food Hydrocolloid.* **2005**, *19*, 303.
32. Mosmann, T. *J. Immunol. Methods* **1983**, *65*, 55.
33. Liu, Z.; Ge, X.; Lu, Y.; Dong, S.; Zhao, Y.; Zeng, M. *Food Hydrocolloid.* **2012**, *26*, 311.
34. Ostrowska-Czubenko, J.; Gierszewska-Drużyńska, M. *Carbohydr. Polym.* **2009**, *77*, 590.
35. Mathew, S.; Brahmakumar, M.; Abraham, T. E. *Biopolymers* **2006**, *82*, 176.
36. Rivero, S.; García, M. A.; Pinotti, A. *Carbohydr. Polym.* **2010**, *82*, 270.
37. Bergo, P.; Sobral, P. J. A. *Food Hydrocolloid.* **2007**, *21*, 1285.
38. Wang, S.-F.; Shen, L.; Zhang, W.-D.; Tong, Y.-J. *Biomacromolecules* **2005**, *6*, 3067–3072.
39. Lima, C. G. A.; de Oliveira, R. S.; Figueiró, S. D.; Wehmann, C. F.; Góes, J. C.; Sombra, A. S. B. *Mater. Chem. Phys.* **2006**, *99*, 284–288.
40. Lavorgna, M.; Piscitelli, F.; Mangiacapra, P.; Buonocore, G. G. *Carbohydr. Polym.* **2010**, *82*, 291–298.
41. Sionkowska, A.; Wisniewski, M.; Skopinska, J.; Kennedy, C. J.; Wess, T. J. *Biomaterials* **2004**, *25*, 795–801.
42. Ogawa, K.; Yui, T.; Okuyama, K. *Int. J. Biol. Macromol.* **2004**, *34*, 1–8.
43. Bigi, A.; Panzavolta, S.; Rubini, K. *Biomaterials* **2004**, *25*, 5675–5680.
44. Chen, C.-H.; Wang, F.-Y.; Mao, C.-F.; Liao, W.-T.; Hsieh, C.-D. *Int. J. Biol. Macromol.* **2008**, *43*, 37–42.
45. Meng, X.; Tian, F.; Yang, J.; He, C.-N.; Xing, N.; Li, F. *J. Mater. Sci.: Mater. Med.* **2010**, *21*, 1751.
46. Tsukada, M.; Shiozaki, H.; Freddi, G.; Crighton, J. S. *J. Appl. Polym. Sci.* **1997**, *64*, 343.
47. Suyatma, N. E.; Tighzert, L.; Copinet, A.; Coma, V. *J. Agric. Food. Chem.* **2005**, *53*, 3950.
48. Apostolov, A. A.; Fakirov, S.; Vassileva, E.; Patil, R. D.; Mark, J. E. *J. Appl. Polym. Sci.* **1999**, *71*, 465.
49. Dai, C.-A.; Chen, Y.-F.; Liu, M.-W. *J. Appl. Polym. Sci.* **2006**, *99*, 1795.
50. Langmaier, F.; Mokrejs, P.; Kolomaznik, K.; Mladek, M. *Thermochim. Acta* **2008**, *469*, 52.
51. Patil, R. D.; Mark, J. E.; Apostolov, A.; Vassileva, E.; Fakirov, S. *Eur. Polym. J.* **2000**, *36*, 1055.
52. Uriarte-Montoya, M. H.; Arias-Moscoso, J. L.; Plascencia-Jatomea, M.; Santacruz-Ortega, H.; Rouzaud-Sández, O.; Cardenas-Lopez, J. L.; Marquez-Rios, E.; Ezquerra-Brauer, J. M. *Bioresour. Technol.* **2010**, *101*, 4212.
53. Silva, C. L.; Pereira, J. C.; Ramalho, A.; Pais, A. A. C. C.; Sousa, J. J. S. *J. Membr. Sci.* **2008**, *320*, 268.
54. Peña, C.; de la Caba, K.; Eceiza, A.; Ruseckaite, R.; Mondragon, I. *Bioresour. Technol.* **2010**, *101*, 6836.
55. Dawson, R. M. C.; Elliott, D. C.; Elliott, W. H. In Data for Biochemical Research, 3rd ed.; Oxford University Press: Oxford, **1989**.
56. Jiang, Y.; Li, Y.; Chai, Z.; Leng, X. *J. Agric. Food. Chem.* **2010**, *58*, 5100.
57. Rhim, J.-W.; Lee, J. H.; Ng, P. K. W. *LWT-Food Sci. Technol.* **2007**, *40*, 232.
58. Martucci, J. F.; Ruseckaite, R. A. *J. Appl. Polym. Sci.* **2009**, *112*, 2166.
59. Ren, D.; Yi, H.; Wang, W.; Ma, X. *Carbohydr. Res.* **2005**, *340*, 2403.
60. Mao, J.; Wang, X.; De Yao, K.; Shang, Q.; Yang, G. *J. Mater. Sci.* **2003**, *38*, 2283.